Journal of Quantitative Spectroscopy & Radiative Transfer 313 (2024) 108838

Contents lists available at ScienceDirect

Journal of Quantitative Spectroscopy and Radiative Transfer

journal homepage: www.elsevier.com/locate/jqsrt

Systematic investigation of transitions to J-mixed Pr I – levels

Laurentius Windholz [a,*], Imran Siddiqui [a,b], Shamim Khan [a,c], Syed Tanweer Iqbal [a,d]

[a] Institute of Experimental Physics, Graz University of Technology, Petersgasse 16, Graz A-8010, Austria
[b] Department of Physics, University of Karachi, University Road, Karachi 75270, Pakistan
[c] Department of Physics, Islamia College Peshawar, KP, Pakistan
[d] Institute of Space Science and Technology (ISST), University of Karachi, University Road, Karachi 75270, Pakistan

ARTICLE INFO

Keywords:
Praseodymium
J-mixed energy levels
New energy levels
Hyperfine structure
Ununsual intensity ratios

ABSTRACT

In JQSRT 305 (2023) 108596 we have recently published the discovery of two energy levels of the Pr atom that exhibit strong J-mixing. Additionally, we present here the manifold of observed hyperfine (hf) structure patterns. Their appearance of these patterns is not solely determined by the J-values of the combining upper levels; the composition of their wave functions also plays a cruical role. In total, we identified 49 transitions involving the J-mixed levels, and laser-spectroscopic investigations were conducted for 46 of them. Notably, 13 upper energy levels are reported for the first time in this study. We hope that this investigation will serve as a catalyst for semi-empirical or ab-initio calculations aimed at explaining these observations.

1. Introduction

During extended work conducted by the laser spectroscopy group at Graz University of Technology, Institute for Experimental Physics, we made a noteworthy discovery of two energy levels. These levels exhibit a unique behavior, resembling both $J = 15/2$ and $J = 13/2$ simultaneously [1]. The historical context of hyperfine (hf) structure investigations on the Praseodymium atom ($Z = 59$; the only stable isotope has mass number 141 and nuclear spin quantum number $I = 5/2$) can be found in the preceding paper [1], and therefore, it will not be reiterated here. The same applies to the experimental particulars. All the spectra presented in this study were acquired by scanning the frequency of narrow-band laser light across a spectral line and observing the resultant laser-induced fluorescence (LIF).

^{141}Pr has a relatively high nuclear magnetic moment and shows a wide hyperfine splitting for many lines, thus in Doppler-limited laser spectroscopy most of the hf components can be resolved and described by the hf structure constants of upper and lower levels. On the other hand, the nuclear electric quadrupole moment of ^{141}Pr is small; thus, only in very rare cases, the electric hyperfine structure constant B leads to noticeable shifts of the hf components. In this paper, with exception of one level, all constants B are treated to be zero.

The energy levels given in [1] are listed in Table 1.

For handling the observed lines and patterns with the classification program "Elements" [2,3] we use 4 auxiliary lower levels, given in Table 2.

The new J-mixing levels are observed only as lower levels of the investigated transitions. We assume they have a metastable character, thus their population in the used source of free Pr atoms (low-density gas discharge) seems to be high. This would also explain the fact that more than 40 transitions to upper levels could be excited by laser light in the relatively small spectral ranges accessible by our laser systems (5583 to 6642 Å and 7092 to 7422 Å). We presume that lot of other transitions could be observed when enlarging these wavelength ranges.

Since the J-mixing levels behave as having $J = 15/2$ and $13/2$ at the same time, we calculated first transition wavelengths to known upper levels having $J_{up} = 11/2$ to $17/2$, corresponding to $\Delta J = 0, \pm 1$. Setting the laser wavelength to the calculated value, we searched for LIF lines. If we found such signal, we scanned the laser frequency across the line and recorded the hf pattern. But by extending the investigations, we also found transitions to new, not previously known energy levels.

In normal hf patterns, the strongest components are determined by the rule $\Delta F = \Delta J$, and only one group of these components is observed. The observed patterns in which the J-mixed levels are involved do not follow this rule, but we can select the auxiliary level(s) needed to describe the observed hf spectra using this rule.

The observed patterns are named following the observation of the main intense groups of hf components. For example, from $J_{up} = 11/2$ we observe only transitions to $J_{low} = 13/2$, since the rule $\Delta J = \pm 1,0$ holds, and thus to levels {1b} and {2b}. Such a scheme is subsequently named

* Corresponding author.
E-mail address: windholz@tugraz.at (L. Windholz).

https://doi.org/10.1016/j.jqsrt.2023.108838
Received 19 September 2023; Received in revised form 28 October 2023; Accepted 10 November 2023
Available online 11 November 2023

Table 1
Properties of the new J-mixing levels for which J is no good quantum number.

No.	Energy (cm^{-1})	Parity	J	A (MHz)	F	Group in Figures
{1}	15,191.990(10)	odd	15/2+13/2	730(2)	10 to 4	A
{2}	15,191.238(10)	odd	15/2+13/2	666(2)	9 to 4 (no transitions to F=10 observed)	B

Table 2
Auxiliary levels used in the classification program "Elements". The absolute uncertainty of the level energy is 0.010 cm^{-1}, but the energy differences have a much lower uncertainty of 0.002 cm^{-1}.

No.	Energy (cm^{-1})	J	A (MHz)
{1a}	15,192.068	15/2	730(2)
{1b}	15,191.885	13/2	730(2)
{2a}	15,191.381	15/2	666(2)
{2b}	15,191.215	13/2	666(2)

0101. From J_{up} =13/2 we may observe intense groups resembling to transitions to levels {1a},{1b} and {2b}; we name such scheme 1101, and so on. For each of the possible transition schemes, we show one hf pattern (in most cases to the upper level which has the lowest A-factor and thus provides the highest hf splitting).

In Table 3 all observed transitions to the new J-mixing levels are listed. The lower levels are introduced according to Table 2. The transitions are sorted by angular momentum J_{up} of the combining upper levels, and within each J_{up}-group by increasing energy of the upper levels. In column 1 the transitions are numbered, and in column 2 the observed scheme (e.g. 1010, see text before) is given. Columns 3–5 contain information about the upper level (J, energy, hf-constant A), and columns 8–10 contain the same information about the lower level. In column 6 the wavelength of the observed line is given, with two digits after the decimal point, if it is the reading value of our lambdameter (accuracy and resolution 0.01 Å). If three digits after the decimal point are given, the line is visible in the available FT spectrum [4]. Column 7 contains information on the line intensity. If only "nl" is given, it is a new spectral line not reported earlier in the literature, but not appearing in the FT spectrum. If "nl" is followed by a number, the line is visible in the FT spectrum with this signal-to noise ratio (SNR). If only a number is given (e.g. SNR = 40 for transition no. 48), the line was reported already by A. Ginibre [5], but not classified by her.

All A-values given in column 5 for the upper levels were determined within this work under assumption that the lower levels have values $A_{low} = 730$ and $A_{low} = 666$ MHz, respectively. Due to the large number of hf components of the observed patterns, the uncertainty is sometimes lower than reported earlier. In column 11 a reference for the hf constant A of the upper level is given. If the A-value in the cited paper is different from the value given in column 5, the literature value is also given. In most cases the values agree within the given uncertainties. This is not the case for level 31,642.945 cm^{-1} (line no.9), for which we claim to have now a better value. For level 32,512.894 cm^{-1} the uncertainty could be lowered from 15 to 3 MHz.

Some of the upper levels are found during the present investigation. In these cases, the remark "new upper level" is given in column 11. All lines belonging to the new levels can be found in Appendix A. For the new level at 32,420.552 cm^{-1} it was necessary to introduce a relatively large value of the hf constant B (−215 MHz) in order to explain all observed hf patterns.

Lines no.1, 24, 25, and 44 are observed as fluorescence lines when transitions in which the upper levels are involved, were excited by laser light. These lines are outside the wavelength ranges of our dye lasers, and thus their hf patterns could not be recorded. For these transitions, only one lower level from Table 2 is selected. The transition wavelength is calculated for no.24 and no. 44 from the level energies, since the monochromator used for detection of the fluorescence line has a resolution of only ±2 Å and these two lines are not visible in the FT spectrum.

2. Description of the observed patterns

Typical observed hf patterns – all of them show perturbed intensity ratios of the hf components – are presented in Figs. 1-7. In all figures, the experimentally observed patterns are shown in black (traces a). All observed patterns can be well fitted using the levels from Table 3, when allowing arbitrary intensities for the components (traces b in the figures, shown in red). The position and relative intensity of the hf components are shown as bars below trace a. Trace c shows the residual, multiplied by the given factor at the right side of trace c. No larger systematic deviations between experimental and fitted curves were observed. This tells us that the perturbation between the two J-mixed levels influences only the intensities, but not the positions of their hf sublevels.

Simulated patterns, which have theoretical intensity ratios of the hf components, are shown in the figures (trace d) in black if $J_{low} = 13/2$ and in blue if $J_{low} = 15/2$. Below the patterns, their center of gravity (cg) is marked by a vertical line.

In the transition schemes shown in the figures, the transitions are drawn in blue for $\Delta J = J_{low} - J_{up} = -1$, in black for $\Delta J = 0$, and in red for $\Delta J = +1$. If in the experimental trace the weakest components are not observed, the transitions are omitted.

We divide each experimental pattern into group A (transitions to level {1}) and group B (transitions to level {2}). As discussed in ref. [1], we have not observed overlapping hf patterns between the transition to the auxiliary level pairs {1a}, {1b} and {2a}, {2b}. Such overlap would appear for A-values of the upper levels smaller than 300 MHz (the lowest A-value of the upper levels involved here is 395 MHz). Thus, in all drawings shown, the transitions to pair {1a}, {1b} (part A of the figures) are well separated from transitions to {2a}, {2b} (part B of the figures).

Additional information in the figures is the excitation wavelength in Å (integer values) and the A-value of the combining upper level in MHz (left side of trace d). The line numbers corresponding to Table 3 are also given.

2.1. *Upper level having $J_{up} = 11/2$, transition scheme 0101, Fig. 1*

From the transition rule for J it follows that the lower level behaves like having $J_{low} = 13/2$, and only the auxiliary levels {1b} and{2b} are necessary for the description. However, the intensity distributions are quite different compared to regular hf patterns. Since the highest F-value of the upper level is $F_{up} = 8$ and the transition rule $\Delta F = \pm 1,0$ holds, no transitions to $F_{low} = 10$ are observed.

Group A: The transition to level {1b} ($A = 730$ MHz, left part in Fig. 1) should have its highest component for transition $F_{up} - F_{low} = 8 - 9$ (Fig. 1, trace d), and with decreasing F-values of this sequence falling intensities. But in the experiment (trace a) we observe increasing intensity, reaching the maximal value for transition 4 – 5. Transition 3 – 4 then has a little bit lower intensity.

Group B: The calculated hf pattern for transitions to level {2b} looks similar to {1b}, but the spacing of the components is little bit smaller due to the smaller lower A-value (666 MHz) of level {2b}. But for this group the experimental trace has its highest component for the transition $F_{up} - F_{low} = 8 - 9$ as it should be, but the intensities decrease much faster compared to trace d.

Table 3
Observed transitions to the J-mixed levels. The uncertainty of the level energies in col. 4 is 0.010 cm^{-1}, if not otherwise given. E … energy, wl … wavelength, SNR … signal-to-noise-ratio in the FT spectrum, tw … this work. For the level at 32,420.552 cm^{-1} below the value A, the value of hf constant B is given.

		Upper even-parity level			Line		Lower new odd-parity level			
no.	Scheme	J	E (cm^{-1})	A (MHz)	wl (Å)	SNR	J	E (cm^{-1})	A(MHz)	Ref. to upper level
1	2	3	4	5	6	7	8	9	10	11
1	—	11/2	26,222.282	590(3)	9063.358	nl 3	13/2	15,191.885	730(2)	[6]
2	0101	11/2	32,587.304	461(4)	5746.83	nl	13/2	15,191.215	666(2)	new upper level
					5747.05	nl	13/2	15,191.885	730(2)	
3	0101	11/2	32,631.830	466(2)	5732.172	nl 9	13/2	15,191.215	666(2)	new upper level
					5732.39	nl	13/2	15,191.885	730(2)	
4	0101	11/2	32,891.473	395(2)	5648.10	nl	13/2	15,191.215	666(2)	new upper level
					5648.31	nl	13/2	15,191.885	666(2)	
5	0101	13/2	30,371.975	609(3)	6585.462	12	13/2	15,191.215	666(2)	new upper level
					6585.75	nl	13/2	15,191.885	730(2)	
6	1111	13/2	30,834.807	664(2)	6390.624	nl 7	13/2	15,191.215	666(2)	[7] 666(1)
					6390.69	nl	15/2	15,191.381	666(2)	
					6390.90	nl	13/2	15,191.885	730(2)	
					6390.980	nl 5	15/2	15,192.068	730(2)	
7	1101	13/2	31,483.101	601(3)	6136.32	nl	13/2	15,191.215	666(2)	[7] 605(5)
					6136.57	nl	13/2	15,191.885	730(2)	
					6136.64	nl	15/2	15,192.068	730(2)	
8	1101	13/2	31,535.092	505(3)	6116.81	nl	13/2	15,191.215	666(2)	new upper level
					6117.09	nl	13/2	15,191.885	730(2)	
					6117.14	nl	15/2	15,192.068	730(2)	
9	1101	13/2	31,642.945	516(2)	6076.70	nl	13/2	15,191.215	666(2)	[7] 529(2)
					6076.95	nl	13/2	15,191.885	730(2)	
					6077.02	nl	15/2	15,192.068	730(2)	
10	1010	13/2	31,693.804	496(3)	6058.05	nl	15/2	15,191.381	730(2)	new upper level
					6058.31	nl	15/2	15,192.068	730(2)	
11	1101	13/2	31,729.874	431(2)	6044.75	nl	13/2	15,191.215	666(2)	[7] 432(2)
					6045.01	nl	13/2	15,191.885	730(2)	
					6045.07	nl	15/2	15,192.068	730(2)	
12	1101	13/2	31,758.102	504(2)	6034.48	nl	13/2	15,191.215	666(2)	[7] 501(2)
					6034.72	nl	13/2	15,191.885	730(2)	
					6034.79	nl	15/2	15,192.068	730(2)	
13	1101	13/2	31,798.854	556(3)	6019.66	nl	13/2	15,191.215	666(2)	new upper level
					6019.90	nl	13/2	15,191.885	730(2)	
					6019.97	nl	15/2	15,192.068	730(2)	
14	0101	13/2	31,918.774	519(5)	5976.51	nl	13/2	15,191.215	666(2)	new upper level
					5976.75	nl	13/2	15,191.885	730(2)	
15	0101	13/2	32,049.979	530(5)	5930.04	nl	13/2	15,191.215	666(2)	[7]
					5930.24	nl	13/2	15,191.885	730(2)	
16	1010	13/2	32,115.075(25)	594(3)	5907.23	nl	15/2	15,191.381	666(2)	[8] 593(5)
					5907.48	nl	15/2	15,192.068	730(2)	
17	1111	13/2	32,302.560	568(3)	5842.45	nl	13/2	15,191.215	666(2)	[7] 571(3)
					5842.51	nl	15/2	15,191.381	666(2)	
					5842.67	nl	13/2	15,191.885	730(2)	
					5842.73	nl	15/2	15,192.068	730(2)	
18	1010	13/2	32,445.227	666(1)	5794.20	nl	15/2	15,191.381	666(2)	[7]
					5794.44	nl	15/2	15,192.068	730(2)	
19	1111	13/2	32,512.894	593(3)	5771.50	nl	13/2	15,191.215	666(2)	[9] 595(15)
					5771.56	nl	15/2	15,191.381	666(2)	
					5771.72	nl	13/2	15,191.885	730(2)	
					5771.79	nl	15/2	15,192.068	730(2)	
20	1010	13/2	32,608.119	628(3)	5740.04	nl	13/2	15,191.381	666(2)	[9] 620(3)
					5740.27	nl	15/2	15,192.068	730(2)	
21	1110	13/2	32,726.817	565(2)	5701.16	nl	15/2	15,191.381	666(2)	[9] 565(3)
					5701.33	nl	13/2	15,191.885	730(2)	

(*continued on next page*)

Table 3 (*continued*)

		Upper even-parity level			Line		Lower new odd-parity level			
no.	Scheme	J	E (cm^{-1})	A (MHz)	wl (Å)	SNR	J	E (cm^{-1})	A(MHz)	Ref. to upper level
1	2	3	4	5	6	7	8	9	10	11
					5701.39	nl	15/2	15,192.068	730(2)	
22	1010	13/2	32,728.757	590(5)	5700.54	nl	15/2	15,191.381	666(2)	new upper level
					5700.76	nl	15/2	15,192.068	730(2)	
23	1111	13/2	32,773.801	838(2)	5685.86	nl	13/2	15,191.215	666(2)	new upper level
					5685.92	nl	15/2	15,191.381	666(2)	
					5686.08	nl	13/2	15,191.885	730(2)	
					5686.145	60	15/2	15,192.068	730(2)	
24	—-	13/2	33,870.147	594(3)	5352.14	nl	13/2	15,191.215	666(2)	[7]
25	—-	15/2	26,654.404	535(1)	8721.829	nl 6	15/2	15,192.068	730(2)	tw
26	0101	15/2	28,661.560(15)	551(2)	7421.670	nl 3	13/2	15,191.215	666(2)	[10] 550(2)
				551(2)	7422.040	nl 3	13/2	15,191.885	730(2)	
27	1110	15/2	29,287.637	512(3)	7092.130	nl 9	15/2	15,191.381	666(2)	[10] 510(3)
				512(3)	7092.38	nl	13/2	15,191.885	730(2)	
				512(3)	7092.471	nl 12	15/2	15,192.068	730(2)	
28	1101	15/2	30,242.928(25)	463(3)	6641.92	nl	13/2	15,191.215	666(2)	[8] 462(5)
				463(3)	6642.22	nl	13/2	15,191.885	730(2)	
				463(3)	6642.31	nl	15/2	15,192.068	730(2)	
29	0101	15/2	30,283.139	477(3)	6624.22	nl	13/2	15,191.215	666(2)	[9] 475(5)
				477(3)	6624.51	nl	15/2	15,192.068	730(2)	
30	1111	15/2	30,959.764	572(3)	6339.981	18	13/2	15,191.215	666(2)	[10] 573(5)
				572(3)	6340.25	nl	15/2	15,191.381	666(2)	
				572(3)	6340.25	nl	13/2	15,191.885	730(2)	
				572(3)	6340.32	nl	15/2	15,192.068	730(2)	
31	1111	15/2	31,070.554	551(2)	6295.74	nl	13/2	15,191.215	666(2)	[10]
				551(2)	6295.80	nl	15/2	15,191.381	666(2)	
				551(2)	6296.00	nl	13/2	15,191.885	730(2)	
				551(2)	6296.080	nl 16	15/2	15,192.068	730(2)	
32	1101	15/2	31,349.100	608(3)	6187.212	nl	13/2	15,191.215	666(2)	[10] 609(1)
				608(3)	6187.48	nl	13/2	15,191.885	730(2)	
				608(3)	6187.55	nl	15/2	15,192.068	730(2)	
33	0111	15/2	31,402.846	632(2)	6166.700	nl 31	15/2	15,191.381	666(2)	new upper level
				632(2)	6166.78	nl	15/2	15,191.381	666(2)	
				632(2)	6166.957	52	13/2	15,191.885	730(2)	
34	1111	15/2	31,619.936	519(2)	6085.20	nl	13/2	15,191.215	666(2)	[10] 520(2)
				519(2)	6085.26	nl	15/2	15,191.381	666(2)	
				519(2)	6085.45	nl	13/2	15,191.885	730(2)	
				519(2)	6085.52	nl	15/2	15,192.068	730(2)	
35	1101	15/2	31,688.109	732(3)	6060.07	nl	13/2	15,191.215	666(2)	[10] 737(1)
				732(3)	6060.32	nl	13/2	15,191.885	730(2)	
				732(3)	6060.38	nl	15/2	15,192.068	730(2)	
36	0111	15/2	31,744.883	696(2)	6039.29	nl	13/2	15,191.215	666(2)	[10]
				696(2)	6039.353	nl	15/2	15,191.381	666(2)	
				696(2)	6039.54	nl	13/2	15,191.885	730(2)	
37	1110	15/2	32,166.645	507(3)	5889.30	nl	15/2	15,191.381	666(2)	[10] 510(1)
				507(3)	5889.47	nl	13/2	15,191.885	730(2)	
				507(3)	5889.527	nl 12	15/2	15,192.068	730(2)	
38	1111	15/2	32,206.727	551(2)	5875.36	nl	13/2	15,191.215	666(2)	[10] 552(1)
				551(2)	5875.41	nl	15/2	15,191.381	666(2)	
				551(2)	5875.59	nl	13/2	15,191.885	730(2)	
				551(2)	5875.66	nl	15/2	15,192.068	730(2)	
39	0101	15/2	32,336.849	475(2)	5830.76	nl	13/2	15,191.215	666(2)	[9] 475(1)
				475(2)	5830.99	nl	13/2	15,191.885	730(2)	
40	1010	15/2	32,420.552	676(3) −215(10)	5802.51	nl	13/2	15,191.215	666(2)	new upper level B necessary
				676(3) −215(10)	5802.74	nl	15/2	15,192.068	730(2)	
41	1111	15/2	32,486.780	551(2)	5780.23	nl	13/2	15,191.215	666(2)	new upper level
				551(2)	5780.28	nl	15/2	15,191.381	666(2)	

(*continued on next page*)

Table 3 (*continued*)

		Upper even-parity level			Line		Lower new odd-parity level			
no.	Scheme	J	E (cm^{-1})	A (MHz)	wl (Å)	SNR	J	E (cm^{-1})	A(MHz)	Ref. to upper level
1	2	3	4	5	6	7	8	9	10	11
				551(2)	5780.45	nl	13/2	15,191.885	730(2)	
				551(2)	5780.511	nl	15/2	15,192.068	730(2)	
42	1111	15/2	32,658.325	530(2)	5723.46	nl	13/2	15,191.215	666(2)	[10] 531(1)
				530(2)	5723.51	nl	15/2	15,191.381	666(2)	
				530(2)	5723.68	nl	13/2	15,191.885	730(2)	
				530(2)	5723.74	nl	15/2	15,192.068	730(2)	
43	1010	15/2	32,783.940	503(3)	5682.66	nl	15/2	15,191.381	666(2)	[10] 501(3)
				503(3)	5682.88	nl	15/2	15,192.068	730(2)	
44	—-	15/2	33,098.154	480(2)	5583.09	nl	13/2	15,191.885	730(2)	[9]
45	1010	17/2	30,826.745	580(2)	6393.98	nl	15/2	15,191.381	666(2)	[9]
				580(2)	6394.27	nl	15/2	15,192.068	730(2)	
46	1010	17/2	30,848.891	507(2)	6384.945	nl	15/2	15,191.381	666(2)	[9] 507(1)
				507(2)	6385.226	nl	15/2	15,192.068	730(2)	
47	1010	17/2	31,437.355	485(2)	6153.662	18	15/2	15,191.381	666(2)	[10]
				485(2)	6153.925	nl 24	15/2	15,192.068	730(2)	
48	1010	17/2	31,629.427	561(2)	6081.768	55	15/2	15,191.381	666(2)	[10] 563(3)
				561(2)	6082.036	40	15/2	15,192.068	730(2)	
49	1010	17/2	32,472.296	487(3)	5785.12	nl	15/2	15,191.381	666(2)	[10] 489(1)
				487(3)	5785.36	nl	15/2	15,192.068	730(2)	

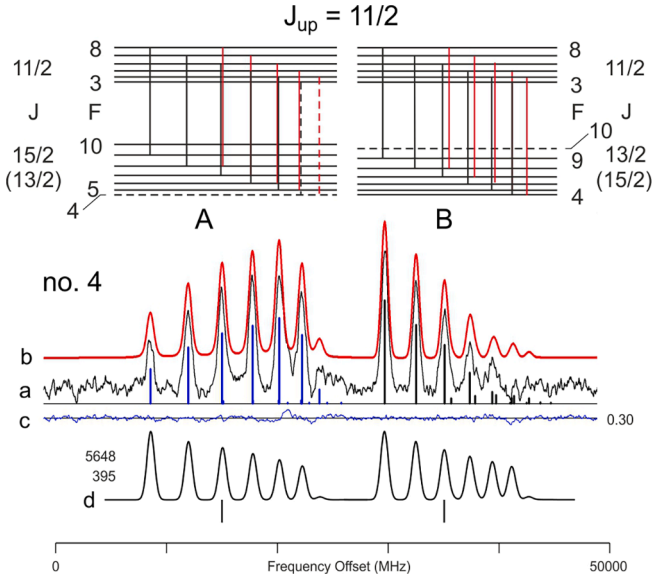

Fig. 1. Transition from an upper level having $J_{up} = 11/2$ (line no.4 in Table 3), transition scheme 0101. (a) experimental record. (b) Fitted curve. (c) Residual between experimental and fitted curve, multiplied with the factor given on the right side. Below trace (a), the hf components are shown as determined in the fit procedure. (d) Simulation of the pattern with theoretical intensity ratios of the hf components. Since the lower level has $J_{low} = 13/2$, the simulation is shown in black. Left of trace (d) the wavelength (in Å as integer value) and the value of the hf constant A of the upper level (in MHz) are given. In the upper part of the figure, the hf level scheme is shown. Since here the highest F-value of the upper level is $F_{up} = 8$ and the transition rule $\Delta F = \pm 1,0$ holds, no transitions to $F_{low} = 10$ are observed.

2.2. Upper levels having $J_{up} = 13/2$ and 15/2

For $J_{up} = 13/2$ and $J_{up} = 15/2$ all possible transition schemes to the four auxiliary levels are observed. For each scheme, the observed patterns show some similarities, independent of the J-value of the upper level.

2.2.1. Transition scheme 0101, Fig. 2

Let us first discuss the case of $J_{up} = 13/2$ and group A. We need only level {1b}, having $J_{low} = 13/2$, for the description of the pattern. The main components are given by $\Delta F = \Delta J = 0$. We observe in principle the same behavior as for the low frequency component group in Fig. 1: In contrary to the theoretical pattern (trace d) the intensity of the

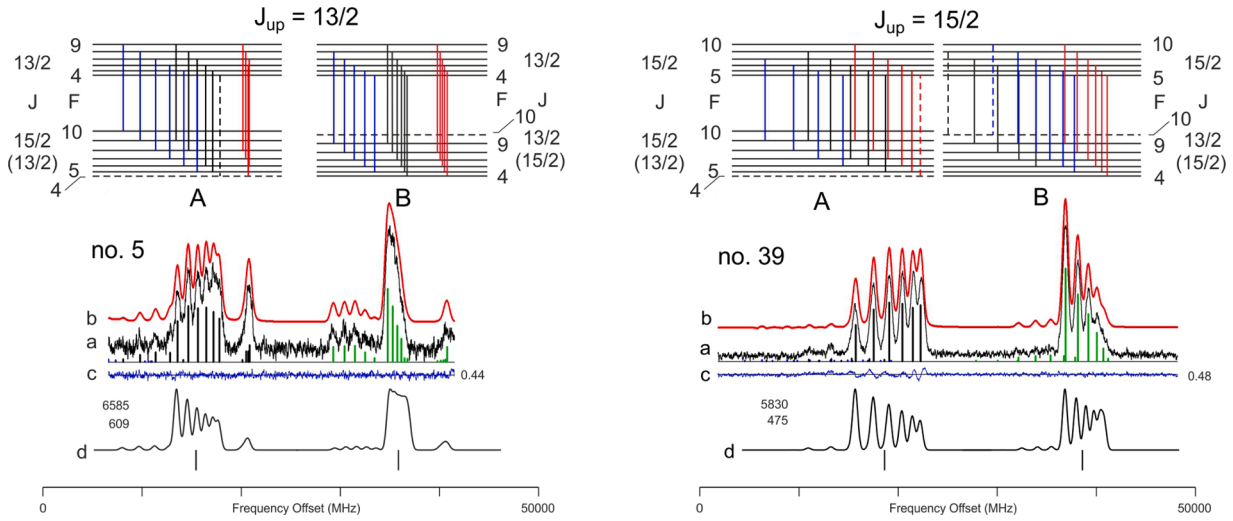

Fig. 2. Transition from upper levels having $J_{up} = 13/2$ (line no.5 in Table 3) and 15/2 (line no.39), respectively, transition scheme 0101. (a) – (d) see Fig. 1. Both lower levels show a behavior like having $J_{low} = 13/2$, but the intensity ratios of the hf components are clearly different from the theoretical ratios. As mentioned in the description of Fig. 1, here the simulated trace is shown in black, since both lower levels have main character $J_{low} = 13/2$.

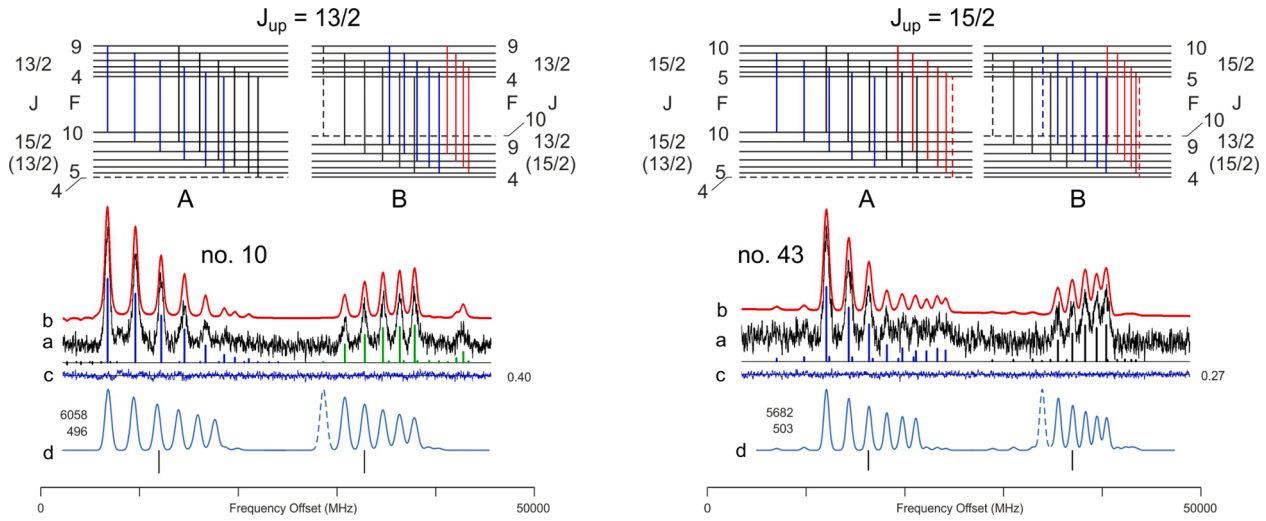

Fig. 3. Transition from upper levels having $J_{up} = 13/2$ (line no.10) and 15/2 (line no.43), respectively, transition scheme 1010. (a) – (d) see Fig. 1. Both lower levels show a behavior like having $J_{low} = 15/2$. Again, the intensity ratios of the hf components are clearly different from the theoretical ratios. Here the simulated trace is shown in blue, since both lower levels have main character 15/2. The transitions to lower level {2a} (group B) are observed without the largest theoretical component (to $F_{low} = 10$). At the transition from $J_{up} = 13/2$, the small peaks at the highest offset frequency are at the position of transitions having $\Delta F = +1$ (theoretical intensities smaller than 0.01 %).

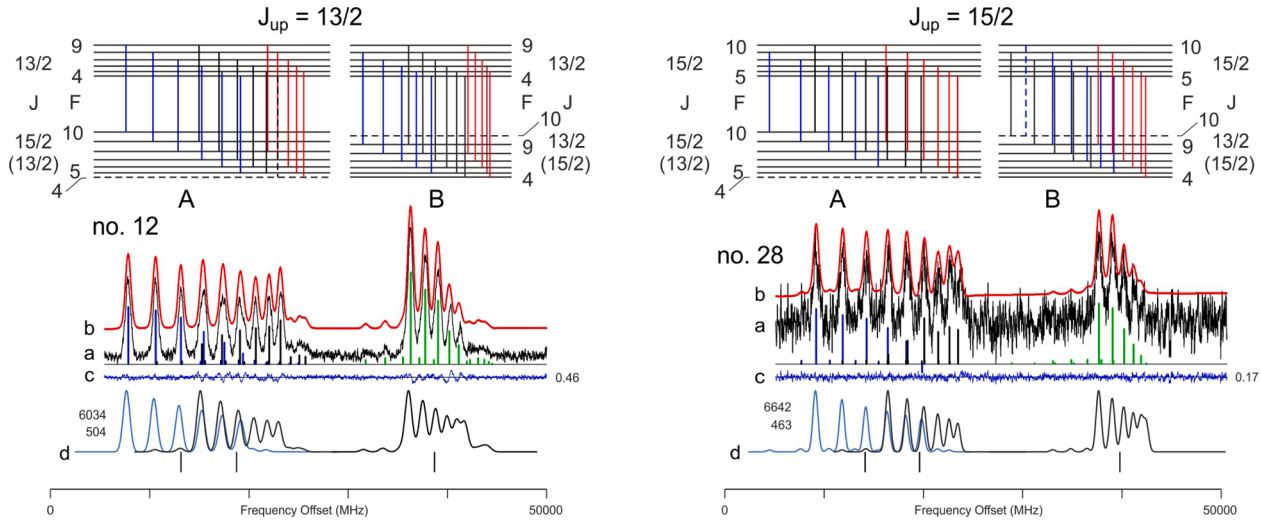

Fig. 4. Transition from upper levels having $J_{up} = 13/2$ (line no.12) and 15/2 (line no.28), respectively, transition scheme 1101. (a) – (d) see Fig. 1. For the description of the low-frequency component group A we need the assumption that transitions to $J_{low} = 15/2$ and 13/2 appear simultaneously (lower levels {1a},{1b}) with approximately the same intensity. The high-frequency groups B are best approximated as transition to $J_{low} = 13/2$ (level {2b}).

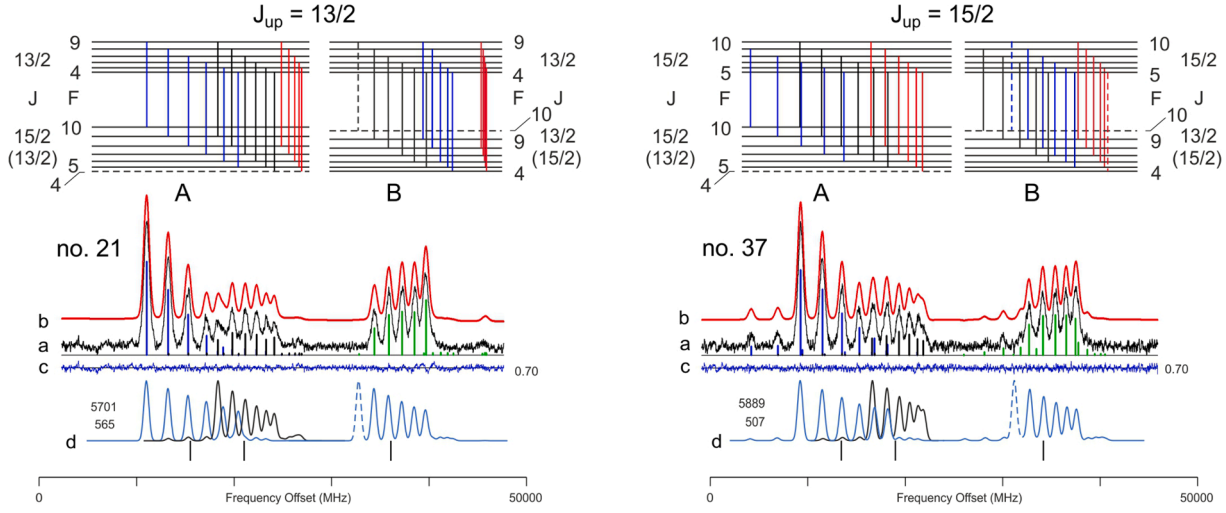

Fig. 5. Transition from upper levels having $J_{up} = 13/2$ (line no.21) and 15/2 (line no.37), respectively, transition scheme 1110. (a) – (d) see Fig. 1. For the description of the low-frequency component group, we need the assumption that transitions to $J_{low} = 15/2$ and 13/2 appear simultaneously (lower levels {1a} and {1b}), but with a different intensity behavior compared to the scheme 1101 (Fig. 4). The high-frequency groups are best approximated as transition to $J_{low} = 15/2$ (level {2a}, without transitions to $F_{low} = 10$).

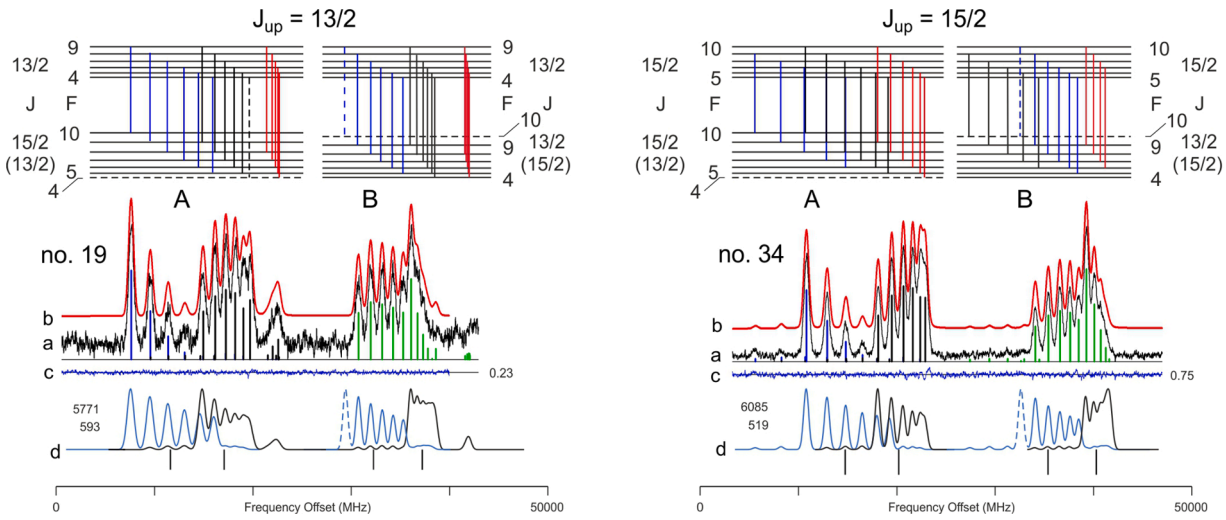

Fig. 6. Transition from upper levels having $J_{up} = 13/2$ (line no.19) and 15/2 (line no. 34), respectively, transition scheme 1111. (a) – (d) see Fig. 1. Here we need all four auxiliary levels to explain the appearance of hf components with high intensities.

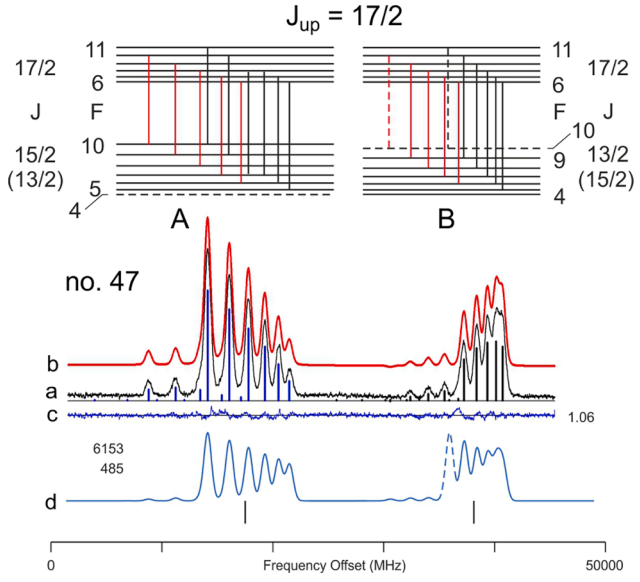

Fig. 7. Transition from an upper level having $J_{up} = 17/2$, transition scheme 1010 (line no.47). (a) – (d) see Fig. 1. Both lower levels show a behavior like having $J_{low} = 15/2$, but the intensity ratios of the hf components are again clearly different from the theoretical ratios. Components with $\Delta F = -1$ have theoretical intensity ratios < 1 % and are not shown, since no corresponding experimental transitions were found.

components is growing instead of decreasing. As usual for transitions having $\Delta J = 0$, components with $\Delta F = +1$ and $\Delta F = -1$ are visible on both sides of the main component group. Due to the relatively large A-value of the upper level ($A_{up} = 609$ MHz), the $\Delta F = -1$ components overlap and form an intense peak. $J_{up} = 13/2$, group B: The transitions to level {2b} show more or less regular intensity distribution, but with a much faster intensity decrease within the $\Delta F = 0$ group.

With the upper level having $J_{up} = 15/2$, the patterns look quite similar, but the role of the $\Delta F = 0$ group in the case of $J_{up} = 13/2$ is now played by the groups $\Delta F = -1$, and the component group $\Delta F = +1$ is not noticeable in the experimental trace.

2.2.2. *Transition scheme 1010, Fig. 3*

In contrary to the pattern discussed in paragraph 2.2.1, here the transitions to $J_{low} = 15/2$ dominate. $J_{up} = 13/2$, group A: The observed experimental pattern (trace a) is close to the theoretical one (trace d), but with decreasing F-values the intensity decrease is much faster. For group B the intensities of the components are increasing instead of decreasing, and the transition to $F_{low} = 10$ is missing.

$J_{up} = 15/2$: In group A now on both sides of the group of strong components weaker components with $\Delta F = \pm 1$ are visible. Group B behaves similar as for $J_{up} = 13/2$. Again no transition to $F_{low} = 10$ could be found.

2.2.3. *Transition scheme 1101, Fig. 4*

Here for the description of group A we need both lower levels, {1a} and {1b}, while for group B only lower level {2b} is required. All components of group A have approximately the same intensity.

2.2.4. *Transition scheme 1110, Fig. 5*

As discussed in Section 2.2.3, we need both lower levels, {1a} and {1b}, for the description of group A, while in group B only lower level

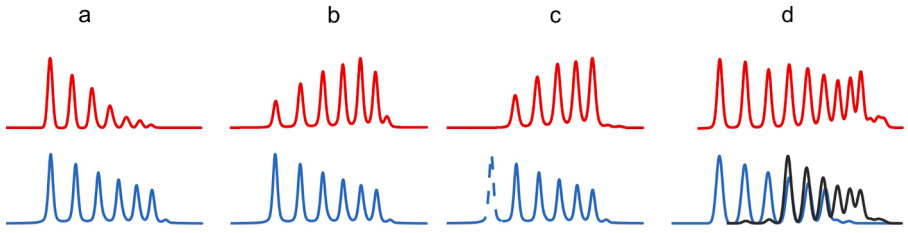

Fig. 8. Main types of observed most intense hf component groups. Explanation see text. Red: simulation of the experimentally observed patterns. For comparison patterns with theoretical intensity rations are show. For the types a-c $J_{low} = 15/2$ (blue) was assumed; for type d we need both, $J_{low} = 15/2$ and 13/2 (black).

Table 4
Observed types and their appearance in the figures.

Fig.	scheme	J_{up}, group	J_{low}	level no.	ΔJ	ΔF
Type a: Strong decrease of the intensities of the main component group						
1	0101	11/2, B	13/2	{2b}	+1	+1
2	0101	13/2, B	13/2	{2b}	0	0
2	0101	15/2, B	13/2	{2b}	−1	−1
3	1010	13/2, B	15/2	{1a}	+1	+1
3	1010	15/2, A	15/2	{1a}	0	0
4	1101	13/2, B	13/2	{2b}	0	0
4	1101	15/2, B	13/2	{2b}	−1	−1
5	1110	13/2, A	15/2	{1a}	+1	+1
5	1110	15/2, A	15/2	{1a}	0	0
6	1111	13/2, A	15/2	{1a}	+1	+1
6	1111	13/2, B	13/2	{2b}	0	0
6	1111	15/2, A	15/2	{1a}	0	0
6	1111	15/2, B	13/2	{2b}	−1	−1
7	1010	17/2, A	15/2	{1a}	−1	−1
Type b: Increase and decrease of the intensities in the main component group						
1	0101	11/2, A	13/2	{1b}	+1	+1
2	0101	13/2, A	13/2	{1b}	0	0
2	0101	15/2, A	13/2	{1b}	−1	−1
5	1110	13/2, A	13/2	{2b}	0	0
5	1110	15/2, A	13/2	{2b}	−1	−1
6	1111	13/2, A	13/2	{2b}	0	0
6	1111	15/2, A	13/2	{2b}	−1	−1
Type c: Increase of the intensities in the main component group, without transition to $F_{low} = 10$						
3	1010	13/2, B	15/2	{2a}	+1	+1
3	1010	15/2, B	15/2	{2a}	0	0
5	1110	13/2, B	15/2	{2a}	+1	+1
5	1110	15/2, B	15/2	{2a}	0	0
6	1111	13/2, B	15/2	{2a}	+1	+1
6	1111	15/2, B	15/2	{2a}	0	0
7	1010	17/2, B	15/2	{2a}	−1	−1
Type d: Nearly uniform component intensity						
4	1101	13/2, A	15/2, 13/2	{1a}, {1b}	+1, 0	+1, 0
4	1101	15/2, A	15/2, 13/2	{1a}, {1b}	0, −1	0, −1

{2a} is present. In contrary to scheme 1101, the transitions to {1a} show a fast decrease of the intensities, and to {1b} nearly same but smaller intensities. The intensities of the components in group B show an increase in intensities, in contrary to the theoretical pattern.

2.2.5. *Transition scheme 1111, Fig. 6*

Here we need all four auxiliary levels for the best description of the observed patterns. In group A transitions to auxiliary level {1a} shows fast decreasing intensities, to level {1b} increasing intensities. In group B both transitions to {2a} and {2b} are present with high intensities. Components to {2a} show increasing intensities compared to the theoretical pattern, and transitions to {2b} a much faster decrease.

2.3. *Upper level having $J_{up} = 17/2$, transition scheme 1010, Fig. 7*

In this case, only transitions to lower levels having $J_{low} = 15/2$ are observed ({1a},{2a}). Compared to transitions from $J_{up} = 11/2$ (Fig. 1), the observed patterns of groups A and B are now exchanged.

3. Types of most intense patterns

In Figs. 1-7 we observe some generalized types of most intense hf patterns. These types are depicted in Fig. 8.

3.1. *Type a*

Strong decrease of the intensities of the main component group. Here the hf components show more or less usual behavior, but, compared to theoretical intensity ratios, the intensities of the components are decreasing much faster with decreasing quantum numbers F.

3.2. *Type b*

Increase and decrease of the intensities in the main component group. In contrary to the theoretical pattern, the highest component is not observed at the place where the theoretical pattern has its highest component (highest F-values). Instead, the intensities are first increasing and reach most intensity at the last minus one component. The last component then has little lower intensity. This type is observed at transitions within group A (to levels {1a},{1b}).

3.3. *Type c*

For transitions to level {2a}) within group B we never have observed transitions to $F_{low} = 10$. The intensities grow like for type b, but here, the last component is the most intense one.

3.4. *Type d*

For the transition scheme 1101, a nearly uniform intensity of the hf components within group A (transitions to levels {1a} and {1b}) is observed.

The types and their appearance in the figures, together with values ΔJ and ΔF, are listed in Table 4.

4. Comments on the interpretation of the spectra

In ref. [1] we have discussed also other possibilities of interpretation

Table 5
Observed transitions in which the newly found energy levels are involved (transitions to the J-mixed levels: see Table 3). E … energy, wl … wavelength, C … comment: nl … new line, cl … known line which could be classified, f … line observed as fluorescence line after laser excitation, e … laser excited transition, SNR … signal-to-noise-ratio in the FT spectrum. "-" in col. 6 means that the line is not visible in the FT spectrum or hidden in a complicated blend situation. For the level at 32,420.552 cm^{-1}, below the A-value the value of hf constant B is given.

New even-parity level			Line			Combining odd-parity level				
J	E (cm^{-1})	A (MHz)	wl (Å)	C	SNR	J	E (cm^{-1})	A (MHz)	B (MHz)	Ref. to A, B comment
1	2	3	4	5	6	7	8	9	10	11
11/2	32,587.304	461(4)	3203.104	nl, f	2	11/2	1376.602	730.393	−11.877	[11]
			4702.880	cl, f	10	9/2	11,329.696	530(3)	-	[12], Blend
			4855.330	cl, f	6	11/2	11,997.137	585(3)	-	[12], Blend
			6144.90	nl, e	-	13/2	16,318.118	281(2)	-	[12]
			6184.50	nl, e	-	11/2	16,422.282	605(3)	-	[12]
11/2	32,631.830	466(2)	5693.11	nl, e	-	9/2	15,071.618	635(3)	-	[12]
11/2	32,891.473	395(2)	4634.98	nl, f	-	11/2	11,322.443	1272(1)	75(50)	[12]
			4784.6474	cl, f	6	11/2	11,997.137	585(3)	-	[12]
			5438.81	nl, f	-	13/2	14,510.207	1085(2)	-	[12]
			5593.366	nl, e	5	13/2	15,018.088	108(3)	-	[12], Blend
			5714.22	nl, e	-	9/2	15,396.135	719(2)		[6]
			5799.785	nl, e	7	13/2	15,654.235	577(1)		[7] Blend
13/2	30,371.975	609(3)	3447.838	nl	31	11/2	1376.602	730.393	−11.877	[11]
			3631.995	nl	7	13/2	2846.741	613.240	−12.850	[11]
			5008.312	cl, f	8	13/2	10,410.745	656(1)	−30(20)	[13]
			5387.207	cl, f	13	15/2	11,814.647	355(2)	0(10)	[12], Blend
			5876.76	nl, e	-	11/2	13,360.511	151(3)	-	[12], Blend
			6107.159	cl, f	21	11/2	14,002.294	566(1)	−125(50)	[12]
			6191.866	cl, e	24	11/2	14,226.220	869(3)	-	[12], Blend
			6302.73	nl, f	-	13/2	14,510.207	1085(2)	-	[12], Blend
13/2	31,535.092	505(3)	3314.865	nl. f	3	11/2	1376.602	730.393	−11.877	[11]
			3484.74	nl, f	-	13/2	2846.741	613.240	−12.850	[11]
			3681.65	nl, f	-	15/2	4381.072	541.575	−14.558	[11]
			5069.47	nl, f	-	15/2	11,814.647	355(2)	0(10)	[12], Blend
			5116.8167	cl, f	70	11/2	11,997.137	585(3)	-	[12]
			5394.26	nl, f	-	15/2	13,002.023	317(2)	30(50)	[12], Blend
			5563.414	nl, f	15	15/2	13,565.490	917(1)	10(10)	[12], Blend
			5702.015	cl, e	22	11/2	14,002.294	566(1)	−125(50)	[12]
			5775.789	nl, e	8	11/2	14,226.220	869(3)	-	[12], Blend
			5872.132	nl, f	-	13/2	14,510.207	1085(2)	-	[12]
			5962.96	nl, f	-	15/2	14,769.529	806(2)	-	[12]
			6052.69	nl, f	-	13/2	15,018.088	108(3)	-	[12]
			6195.60	nl, f	-	15/2	15,399.063	889(2)	-	[12]
13/2	31,693.804	496(3)	3297.509	nl	5	11/2	1376.602	730.393	−11.877	[11], Blend
			5075.5868	cl, f	130	11/2	11,997.137	585(3)	-	[12], Blend
			5892.87	cl, e	-	11/2	14,728.843	811(2)	-	[12]
13/2	31,798.854	556(3)	5617.504	cl, f	25	11/2	14,002.294	566(1)	−125(50)	[12], Blend
			5957.5537	cl	11	13/2	15,018.088	108(3)	-	[12], Blend
13/2	31,918.774	519(5)	5018.268	cl, f	116	11/2	11,997.137	585(3)	-	[12]
13/2	32,728.757	590(5)	5566.622	nl, f	15	15/2	14,769.529	806(2)	-	[12], Blend
			6270.233	nl	4	15/2	16,784.797	297(5)		[10], Blend
13/2	32,773.801	838(2)	3184.0765	nl, f	8	11/2	1376.602	730.393	−11.877	[11]
			4470.41	nl, f	-	13/2	10,410.745	656(1)	−30(20)	[13]
			5473.85	nl, f	-	13/2	14,510.207	1085(2)	-	[12]
			5540.175	nl, f	5	11/2	14,728.843	811(2)	-	[12], Blend
			5568.79	nl, e	-	11/2	14,821.570	544(2)		[12]
			5952.02	nl, e	-	11/2	15,977.45	66(3)	-	[12]
15/2	31,402.846	632(2)	5743.251	nl, e	3	13/2	13,995.931	1067(1)	200(50)	[12], Blend
			5918.099	cl, e	20	13/2	14,510.207	1085(2)	-	[12], Blend
			6567.346	nl, e	-	15/2	16,180.200	883(2)		[10], Blend
15/2	32,420.552	676(3)	5223.1643	nl	4	17/2	13,280.404	208(2)	20(50)	[12], Blend hf const. B needed
		−215(15)	6481.1331	cl	22	17/2	16,995.408	992(1)	−50(20)	tw, Blend
15/2	32,486.780	551(2)	3372.846	nl	6	13/2	2846.741	613.240	−12.850	[11]
			5205.161	nl, f	-	17/2	13,280.404	208(2)	20(50)	[12], Blend
			6183.094	nl, e	12	13/2	16,318.118	281(1)	-	[12], Blend
			6366.864	nl	5	15/2	16,784.797	297(5)		[10], Blend

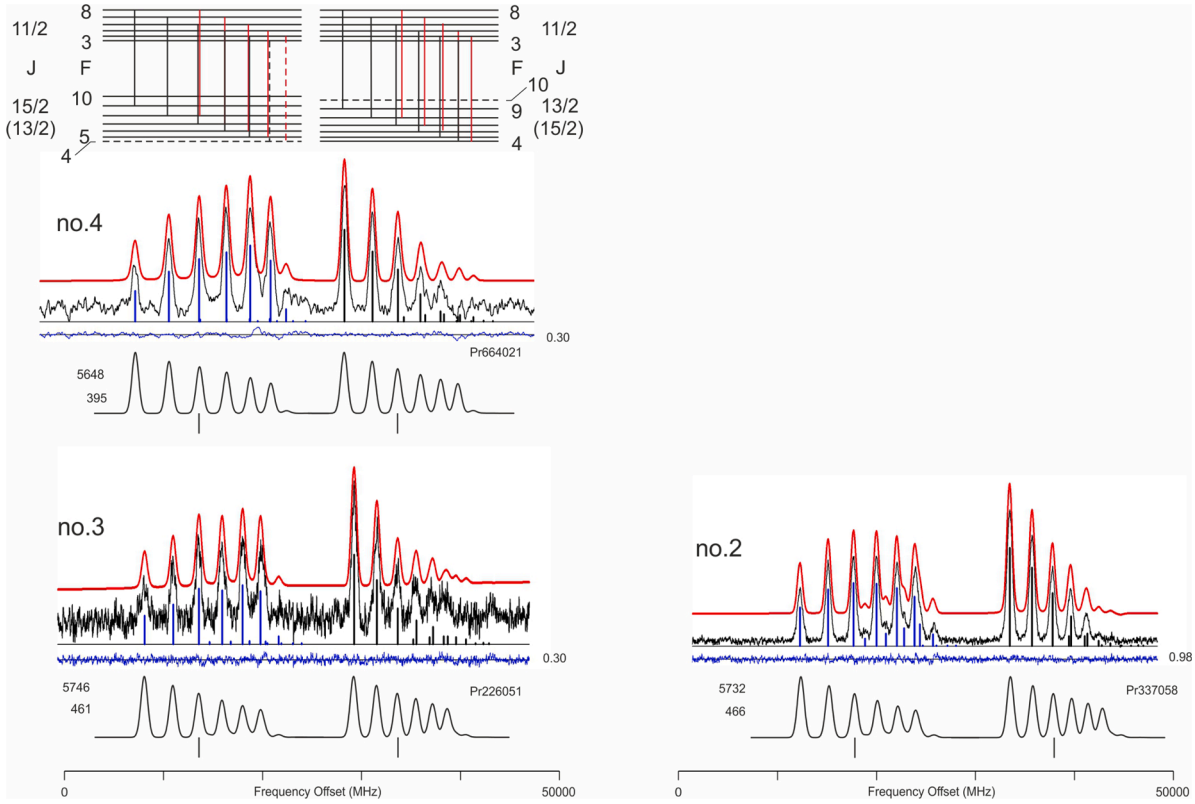

Fig. 9. Transitions from upper levels having $J = 11/2$, transition scheme 0101. For the meaning of the traces see Fig. 1. Additionally, the line numbers from Table 3 are given. Inserted are wavelength (in Å, only integer values) and A-factor of the upper level (in MHz).

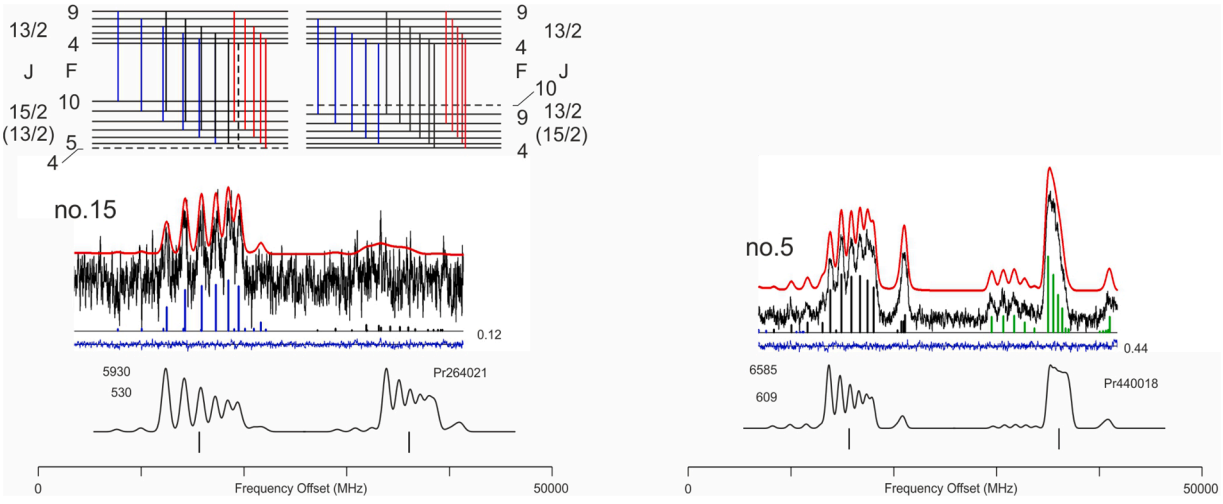

Fig. 10. Transitions from upper levels having $J = 13/2$, transition scheme 0101.

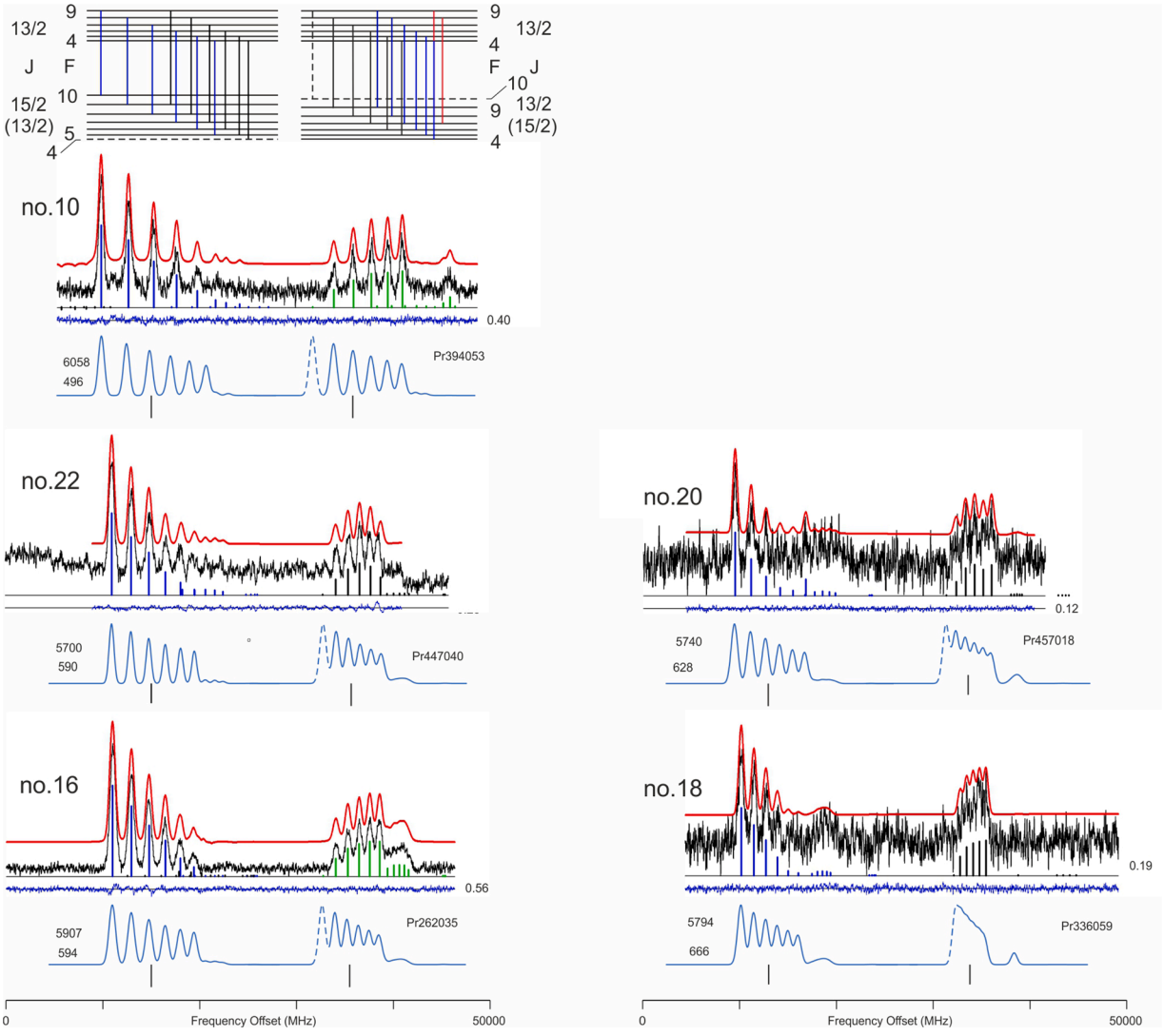

Fig. 11. Transitions from upper levels having $J = 13/2$, transition scheme 1010.

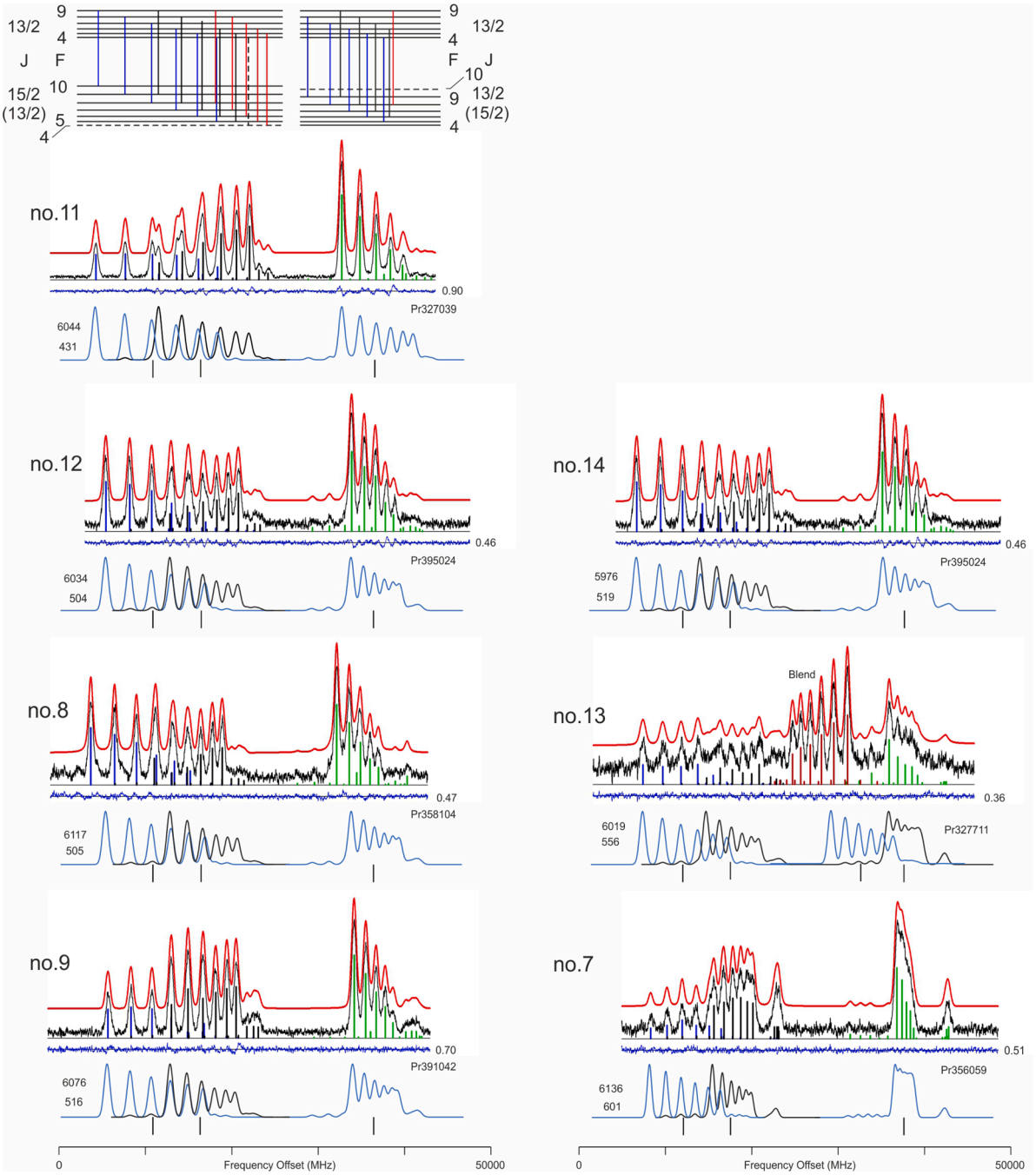

Fig. 12. Transitions from upper levels having $J = 13/2$, transition scheme 1101. In line no.13 between the two transitions discussed here, a blend line is recorded (transition 31,801.951 cm^{-1}, $J_{up} = 17/2$, even parity, $A_{up} = 503(1)$ MHz – 15,194.595 cm^{-1}, $J_{low} = 15/2$, odd parity, $A_{low} = 343(2)$ MHz). Both upper and lower level of the blend line differ in energy by less than 4 cm^{-1} from the levels leading to the structures of line no.13. Thus – due to the limited resolution of the monochromator used in the experiment, an excitation- and a LIF-blend appears.

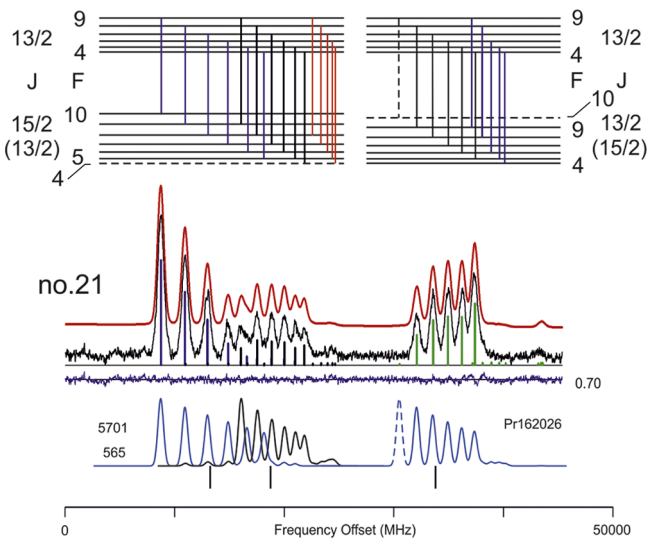

Fig. 13. Transition from an upper level having $J = 13/2$, transition scheme 1110.

of the observed hf spectra. We have excluded that saturation effects are responsible for the observed unusual intensity behavior of the hf components and the possibility, that radationless transitions are responsible for the observations.

In all spectra shown in this study, the frequency position of the observed hf components can be explained with help of the four auxiliary levels. The curves fitting the experimental structures are gained without any conditions for the component intensities, these were free parameters in the fit. Facts that we can state are:

(i) For the description of group A we need F-values of the new level {1} from $F_{low} = 10$ to $F_{low} = 4$, in contradiction to regular levels, while for group B a new level {2} having F_{low}-values between 9 and 4 is necessary. Nevertheless, some patterns of group B are similar to transitions to $J_{low} = 15/2$ (auxiliary level {2a}), but without observation of transitions to $F_{low} = 10$.

(ii) The simulations shown in the figures as traces d correspond to regular hf dipole-transitions. These simulations are shown for comparison only, and we named the spectra (e.g. 1110) after the similarity of the observed to the simulated patterns.

(iii) We cannot exclude that some of the patterns may be better described assuming multipole transitions. A clarification of this point would need extended theoretical investigations which are not available presently.

5. Conclusion

The hf patterns of transitions from upper even-parity energy levels to the J-mixed odd-parity energy levels at 15,191.990(10) and 15,191.238 (10) cm^{-1} (having simultaneously $J = 15/2$ and 13/2) were investigated. Surprisingly, the hf patterns do depend not only on the J-value of the upper levels. It appears that their wave function composition also plays an important role. For $J_{up} = 11/2$ and $J_{up} = 17/2$ the selection of the auxiliary levels, introduced for use of our classification program, follows strictly $\Delta J = \pm 1$. For $J_{up} = 13/2$ and 15/2, several structures, in which two, three or even four of the auxiliary levels are best describing the most intense component groups, were observed. Unfortunately, no recent parametric fit of the wavefunction of Pr levels is available; the only published paper is from the year 2003 [14] and contains calculated hf constants, but not the wavefunction composition of the treated levels. Thus we see an urgent need for new semi-empirical parametric studies of the Pr atom, including all energy levels discovered in the last two decades.

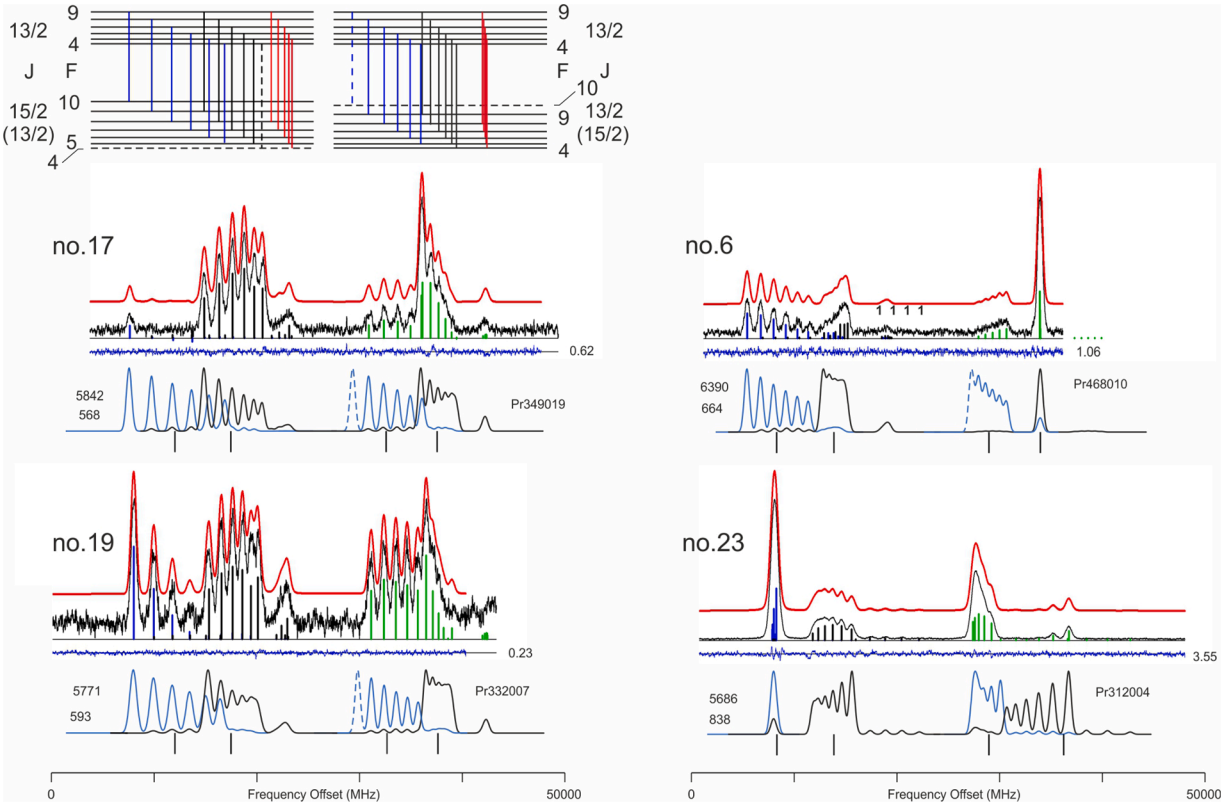

Fig. 14. Transitions from upper levels having $J = 13/2$, transition scheme 1111.

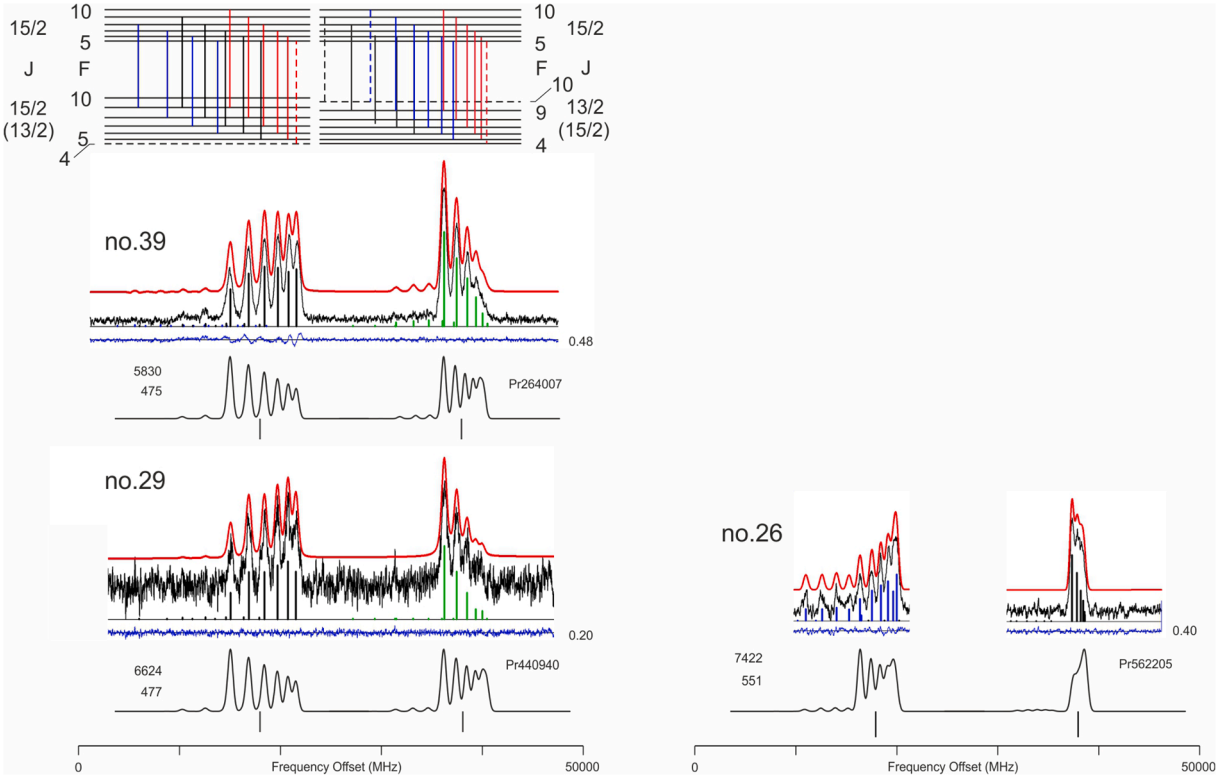

Fig. 15. Transitions from upper levels having $J = 15/2$, transition scheme 0101. For transition no.26, the two parts were recoded separately.

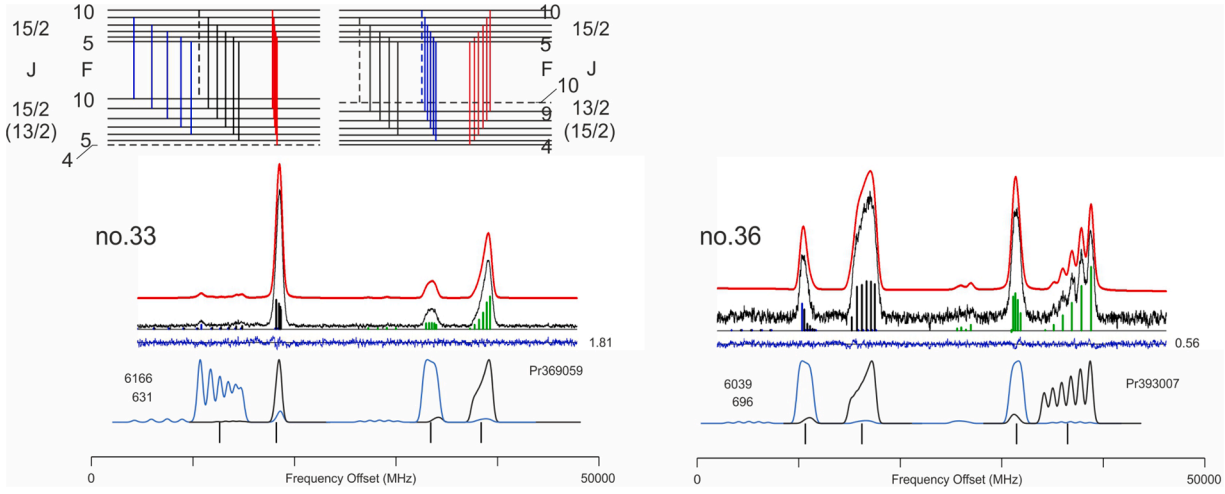

Fig. 16. Transitions from upper levels having $J = 15/2$, transition scheme 0111.

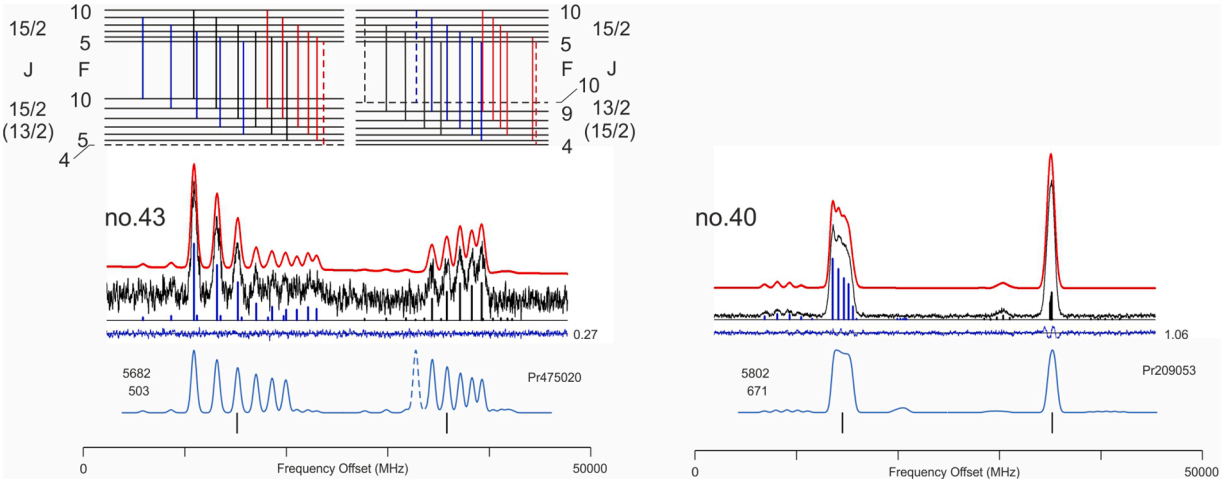

Fig. 17. Transitions from upper levels having $J = 15/2$, transition scheme 1010.

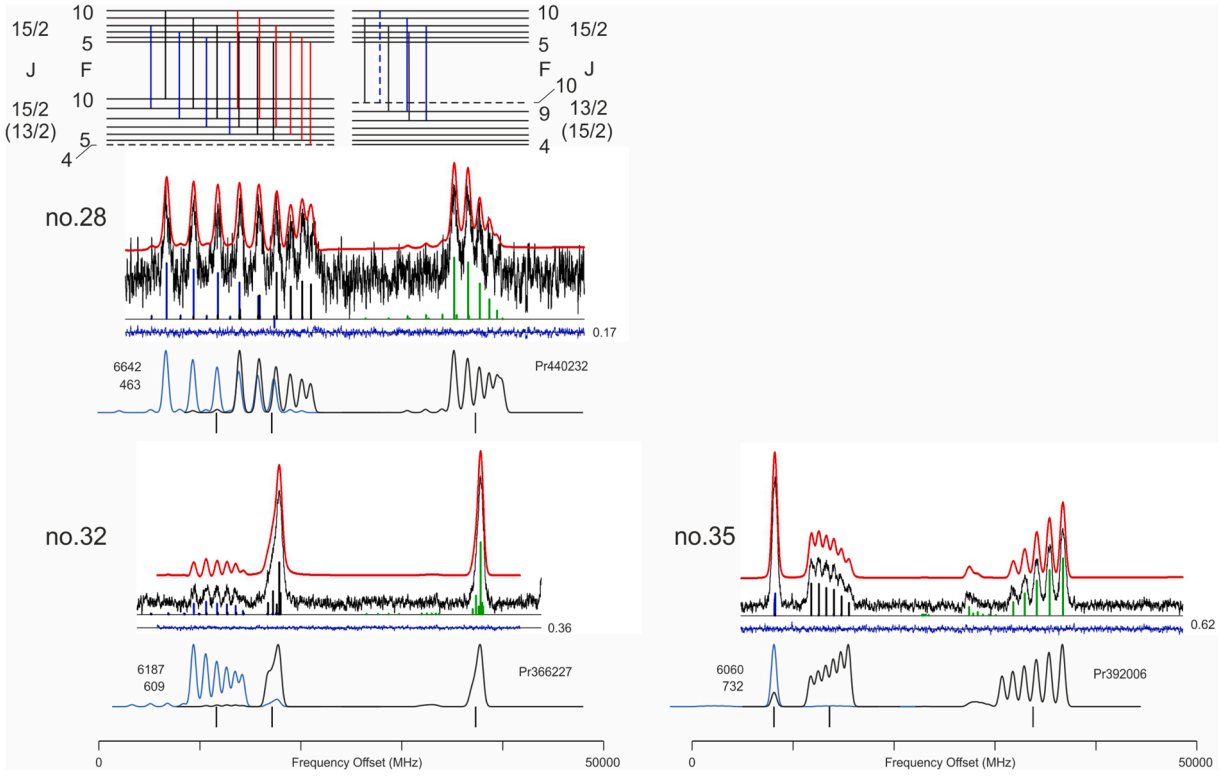

Fig. 18. Transitions from upper levels having $J = 15/2$, transition scheme 1101.

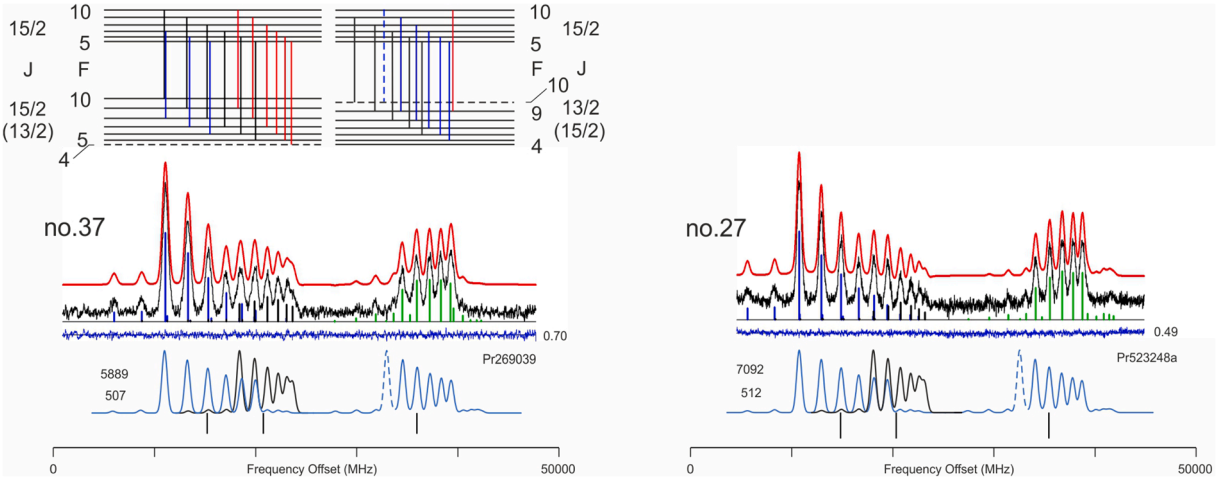

Fig. 19. Transitions from upper levels having $J = 15/2$, transition scheme 1110.

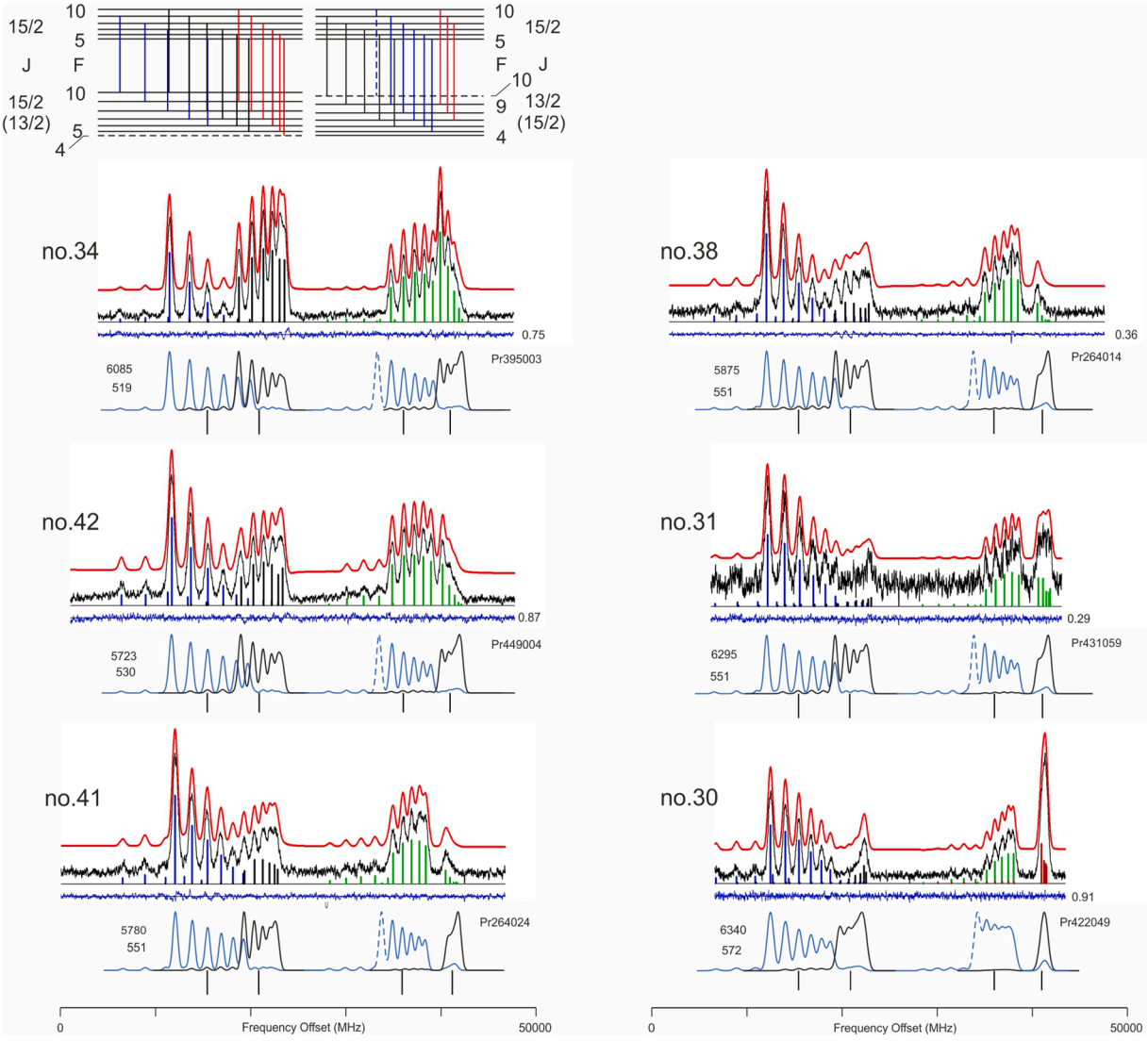

Fig. 20. Transitions from upper levels having $J = 15/2$, transition scheme 1111.

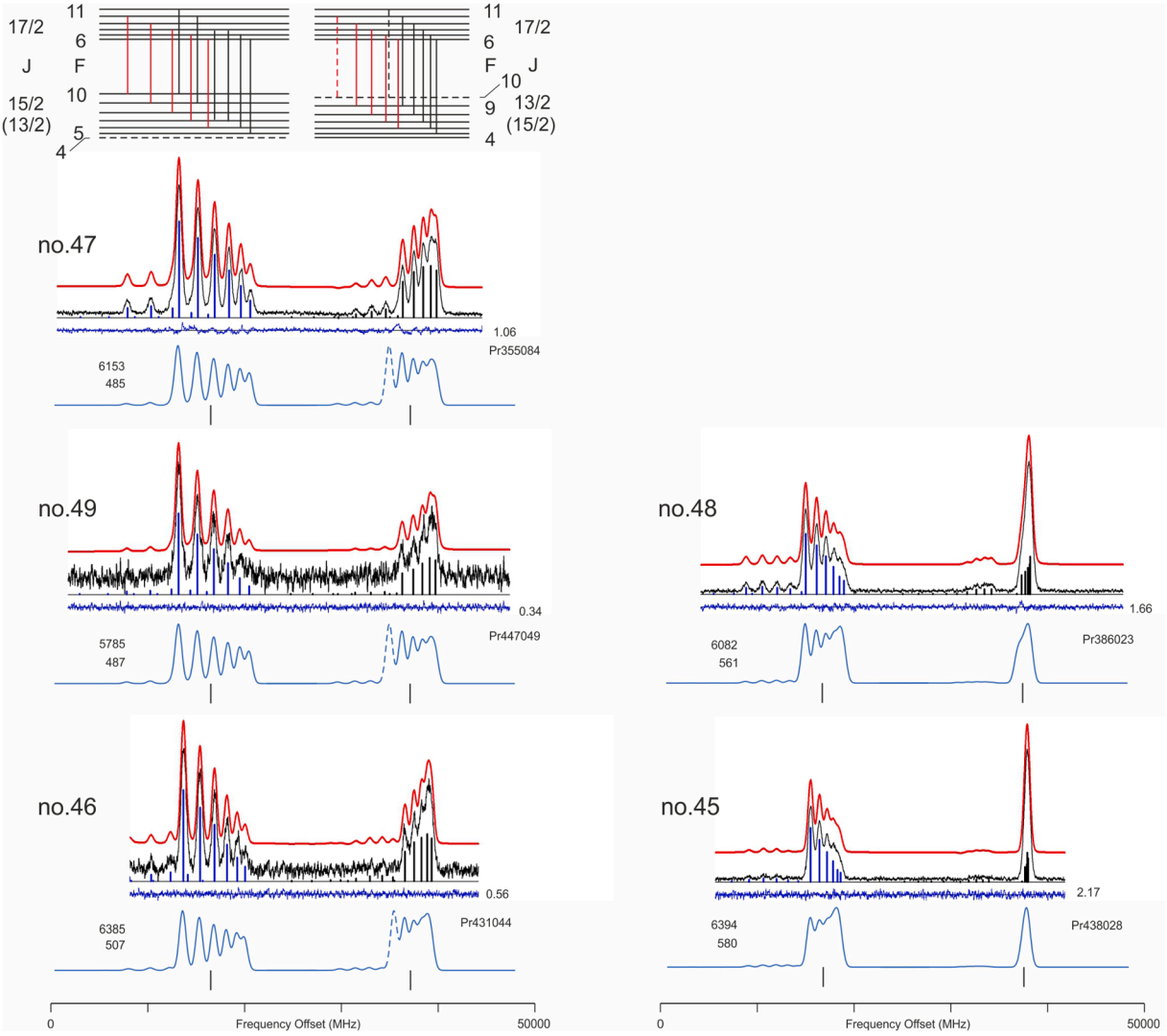

Fig. 21. Transitions from upper levels having $J = 17/2$, transition scheme 1010.

CRediT authorship contribution statement

Laurentius Windholz: Data curation, Writing – original draft, Investigation. **Imran Siddiqui:** Investigation, Writing – review & editing. **Shamim Khan:** Investigation, Writing – review & editing. **Syed Tanweer Iqbal:** Investigation.

Declaration of Competing Interest

The authors declare that they have no known competing financial interests or personal relationships that could have appeared to influence the work reported in this paper.

Data availability

Data will be made available on request.

Acknowledgement

Open Access Funding was provided by Graz University of Technology.

Imran Siddiqui is thankful to the University of Karachi and to Graz University of Technology for providing fundings during his PhD- and PostDoc-periods in Graz. Shamim Khan and Syed Tanweer Iqbal are thankful to the Higher Education Commission (HEC) Pakistan and to Sindh Literacy Department, Government of Sindh, Pakistan.

Appendix A

In Table 5 all observed transitions, in which the newly found energy levels are involved, are listed (with exception of the lines given already in Table 3). The levels are arranged due to their angular momentum J_{up}, and within each group by increasing energy. The uncertainty of the energies is 0.010 cm^{-1}. The wavelength values in col. 4 are calculated from the level energies or come from the reading of our lambdameter (accuracy ± 0.01 Å), if two digits after the decimal point are given. For lines which wavelength could be determined from the FT spectrum, three or four digits after the decimal point are given.

Appendix B

In the appendix the hf patterns of all transitions, for which laser excitation was successful, are shown (Figs. 9 to 21). If for one type (e.g. 0101) several lines are observed, they are sorted by increasing A-factor of the upper level. The splitting of two hf components having the same value ΔF decreases with increasing value of A_{up}, if A_{low} is the same. If the value of A_{up} is close to A_{low}, some components are overlapping. A level

scheme is given only for the line with the smallest value of A_{up} (largest splitting of the hf components).

References

[1] Siddiqui I, Windholz L. Experimental evidence for the existence of two neighboring Pr I energy levels for which J is not a good quantum number. JQSRT 2023;305: 108596. https://doi.org/10.1016/j.jqsrt.2023.108596.

[2] Windholz L, Guthöhrlein GH. Classification of spectral lines by means of their hyperfine structure. application to Ta I and Ta II levels. Physica Scripta 2003;T105: 55–60. https://doi.org/10.1238/Physica.Topical.105a00055.

[3] Windholz L. Finding of previously unknown energy levels using Fourier-transform and laser spectroscopy. Physica Scripta 2016;91:114003. https://doi.org/10.1088/0031-8949/91/11/114003.

[4] Gamper B, Uddin Z, Jahangir M, Allard O, Knöckel H, Tiemann E, Windholz L. Investigation of the hyperfine structure of Pr I and Pr II lines based on highly resolved Fourier transform spectra. J Phys B At Mol Opt Phys 2011;44:045003. https://doi.org/10.1088/0953-4075/44/4/045003 (7pp) with supplementary data.

[5] Ginibre A. [Ph.D. thesis]. Paris: Université de Paris-Sud, Centre d'Orsay; 1988.

[6] Khan S, Siddiqui I, Iqbal ST, Uddin Z, Guthöhrlein GH, Windholz L. Experimental investigation of the hyperfine structure of neutral praseodymium spectral lines and discovery of new energy levels. IJC 2017;9:7–29. https://doi.org/10.5539/ijc.v9n1p7. 23p.

[7] Siddiqui I, Khan S, Windholz L. Experimental investigation of the hyperfine spectra of Pr I-lines: discovery of new fine structure energy levels of Pr I using LIF spectroscopy with medium angular momentum quantum number between 7/2 and 13/2. Eur Phys J D 2016;70:44. https://doi.org/10.1140/epjd/e2016-60485-2. 9p. + supplementary material.

[8] Syed TI, Siddiqui I, Shamim K, Uddin Z, Guthöhrlein GH, Windholz L. New even and odd parity levels of neutral praseodymium. Phys Scr 2011;84(12pp):065303. https://doi.org/10.1088/0031-8949/84/06/065303.

[9] Uddin Z, El Bakkali D, Gamper B, Khan S, Siddiqui I, Guthöhrlein GH, Windholz L. Laser spectroscopic investigations of Praseodymium I transitions: new energy levels. Adv Opt Technol 2012;639126:34. https://doi.org/10.1155/2012/639126.

[10] Siddiqui I, Khan S, Windholz L. Experimental investigation of the hyperfine spectra of Pr I - lines: discovery of new fine structure levels with high angular momentum. Eur Phys J D 2014;68:122. 10 p. + supplement 23 p. 1140/epjd/e2014-50025-7.

[11] Lew H. Hyperfine structure and magnetic moments of Pr141; Bull. Am. Phys. Soc. 15 (1970) 795; values repeated in W.J. Childs, L.S. Goodman; Double resonance, fluorescence spectroscopy, and hyperfine structure in Pr I, Phys. Rev. A 24 (1981) 1342. Doi:10.1103/PhysRevA.24.1342.

[12] Helmut-Schmidt-Universität, Universität der Bundeswehr Hamburg, and Laboratorium für Experimentalphysik, unpublished material taken from several diploma theses (supervisor G. H. Guthöhrlein).

[13] Kuwamoto T, Endo I, Fukumi A, Hasegawa T, Horiguchi T, Ishida Y, Kobayashi T, Kondo T, Takahashi T. Systematic study of fine and hyperfine structures in Pr I by doppler-free atomic beam laser spectroscopy. J Phys Soc Japan 1996;65(10): 3180–5. https://doi.org/10.1143/JPSJ.65.3180.

[14] Ruczkowski J, Stachowska E, Elantkowska M, Guthöhrlein GH, Dembczyński J. Interpretation of the hyperfine structure of the even configuration system of Pr I. J. SPhys Scripta 2003;68:133–40. https://doi.org/10.1238/Physica.Regular.068a00133.